

Reporting Three Unique “Induced Glass Transitions” (IGTs) Appeared in GeSSb Glassy Alloys using DSC

Dipti Sharma^{1*}, Om Sharma², John C MacDonald³, Anjani Kumar⁴,
Rajeev Gupta⁵, Ashok Kumar⁶, Rajendra K Shukla⁶

¹Emmanuel College Boston, MA, USA; ²Natick High School, Natick, MA, USA; ³WPI, Worcester, MA, USA;
⁴Maharana Pratap Engineering College, Kanpur, UP, India; ⁵IIT, Kanpur, UP, India; ⁶HBTU, Kanpur, UP, India.

Abstract:

This research shows some unique detailed results of two chalcogenide GeSSb glassy alloys using Differential Scanning Calorimetry (DSC) technique. The two bulk samples of Ge₂₅S_{75-x}Sb_x (where x = 0% and 5%) were used to run from 0oC to 300 oC for heat and cool in DSC with different ramp rates from 5 oC/min to 40 oC/min. These chalcogenide glasses were made under vacuum of 10⁻⁵ Torr with 12 hours rocking and then quenching technique at HBTU and IIT. It was seen that three multi small endothermic peaks were appeared around 70 – 120 oC in x = 0% which then reappeared with addition of Sb of 5% and got flattened, spread out more widely with lower enthalpy on heating. This appearance is rare and unique in these types of glassy alloys and have not reported in the literature so far. These transitions can be explained in terms of the density of these materials and represents existence of “Induced Glass Transitions (IGTs)” in these glassy alloys.

Keywords: Calorimetry, DSC, glassy alloys, vacuum, heat cool, induced, glass transition, heat flow, temperature, thermodynamics, chalcogenide glasses, ramp rates.

Date of Submission: 20-12-2022

Date of acceptance: 02-01-2023

I. Introduction:

Chalcogenide glassy materials, based on chalcogens (S, Se, Te) are very interesting versatile materials. They exhibit electrical properties, optical properties, photoconductive properties, thermal and dielectric properties. They also have some significant physical properties like high refractive index, low phonon energy, high nonlinearity which makes it ideal for use in lasers, planar optics, photonic integrated circuits, and other active devices [1-5]. Some of these chalcogenide glasses show several non-linear optical effects such as electron induced permittivity modification and photon-induced refraction [6, 7]. Chalcogenide glassy alloys are used in varieties of applications such as infrared detectors, moldable IR optics, IR optical fibers, phase change memory devices, photovoltaic cell, gas sensors, etc. [8-10]. In one of the recent research works, it is shown that chalcogenide has applications in development of thin film-based supercapacitor [1]. A classical chalcogenide glasses such as Ge-S are strong glasses formers and possess glassy materials within large concentration regions, currently various scientists have worked on Ge-S-Sb glassy systems and discovered that these materials can be used in emerging applications such that phase change applications, solid state applications and optical applications [3, 9, 12].

Based on these applications and publications from various authors as mentioned above, our interest is to find some unique properties of Ge-S-Sb glassy alloys that is not discovered yet in the literature. In past, a few studies have found with Ge, GeSe, GeS glasses and their glassy alloys on types of studies including thermal, electrical, dielectric, optical, structural studies. Some studies showed that GeSe or GeS based glasses show slow crystallization and because of being slow structural arrangements, sometimes they do not show Crystallization on heating and skip this transition on heating [13-14]. Our intention is to study GeS glassy alloys with Sb as doping material to see if follow slow crystallization and do not show crystallization in heating or show something new.

Differential Scanning Calorimetry (DSC) technique has been being used in research for decades and decades [15-23]. As time moves further the DSC gets advanced from old fashion to new fashion techniques and shows better thermal curves. Several studies can be seen on thermal properties of matter using DSC [17-23]. Several studies can be found on ramp rates and how sample is heated and cooled [17-23]. Some of these publications show effect of DSC on thermal properties of materials and how ramp rates may affect transitions of the materials. DSC can also be used for slow, moderate, and fast heat and cool. The rate of heat and cool is

considered as ramp rates and these ramp rates may show some unique behavior in the material. We are reporting such a unique result of GeSSb glassy alloys in this paper using DSC.

II. Experimental:

Two glassy alloys of GeSSb Chalcogenide glasses are made at the laboratories IIT Kanpur and HBTU Kanpur India. The form of the alloy contains three elements as $\text{Ge}_{25}\text{S}_{75-x}\text{Sb}_x$ (where $x = 0, 5$) keeping the concentration and proportion of Ge constant and changing S and Sb accordingly to get total 100% of material weight wise. The parent glassy alloy was a binary alloy with GeS and no Sb whereas the next glassy alloy was the ternary glass alloy with GeSSb. The process of making glassy alloys is explained next.

First, High purity (99.9999 %) bulk elements were weighed by electronic balance according to their atomic percentages, with the least count of 10^{-4} gm. The properly weighed materials were then put into clean quartz ampoules (length ~ 5 cm and internal diameter ~ 8 mm). Excess air was pumped out of the ampoule with a diffusion pump in an ampoule sealing station. The sample in the quartz ampoule was sealed under vacuum of about 10^{-5} Torr by carefully melting the opening of the ampoule together with a torch. The vacuum-sealed ampoule was then inserted into a rocking furnace, heated to a desired temperature, and maintained at this temperature for at least 12 hrs so that the amorphous solid will be homogeneous and isotropic. The temperature of the furnace was raised slowly at a rate of 3-4 °C/min. After rocking for about 12 hrs, the obtained molten materials were rapidly quenched by removing the ampoules from the furnace and dropping into ice-cooled water. When the melt had solidified into solid form, the ampoule was wrapped in a protective cloth and carefully cracked opened with a hammer.

It was done in such a way that the alloy was broken along its natural stress line into smaller pieces suitable for grinding and polishing. Then, these glassy alloys were tested by X Ray diffraction technique to make sure that these alloys are glassy not crystalline. Based on the X Ray pattern found, it can be seen in the Figure 1 and Figure 2 that they are glassy amorphous.

X-Ray diffraction pattern of $\text{Ge}_{25}\text{S}_{75-x}\text{Sb}_x$ (where $x = 0, 5$) bulk glasses:

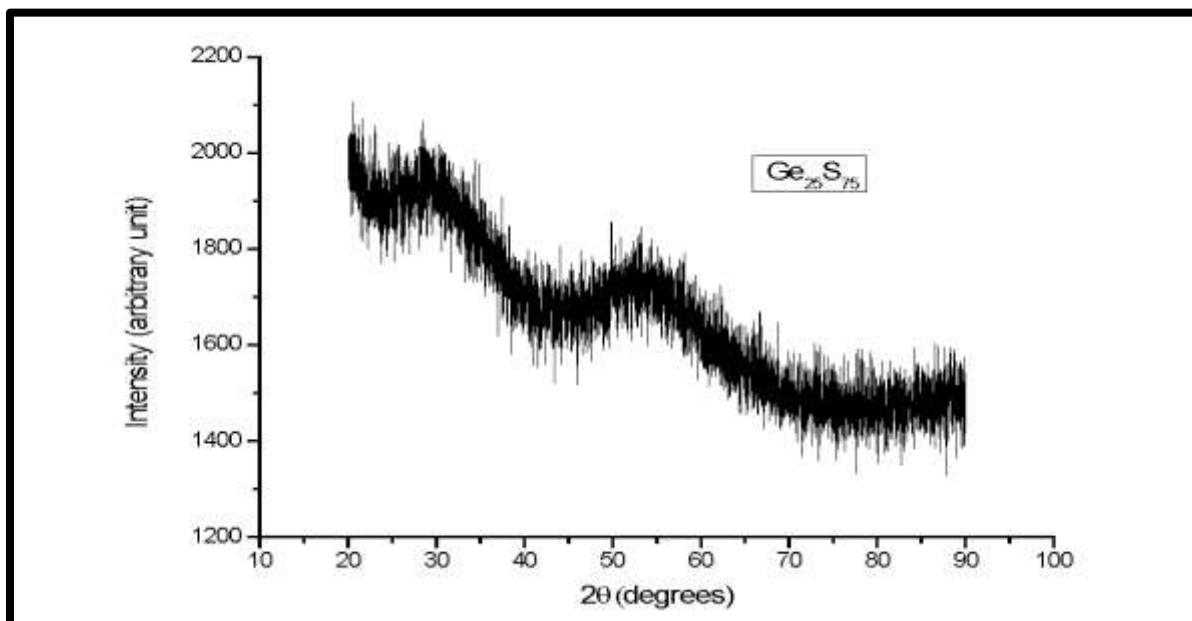


Figure 1: X Ray Diffraction pattern of GeS.

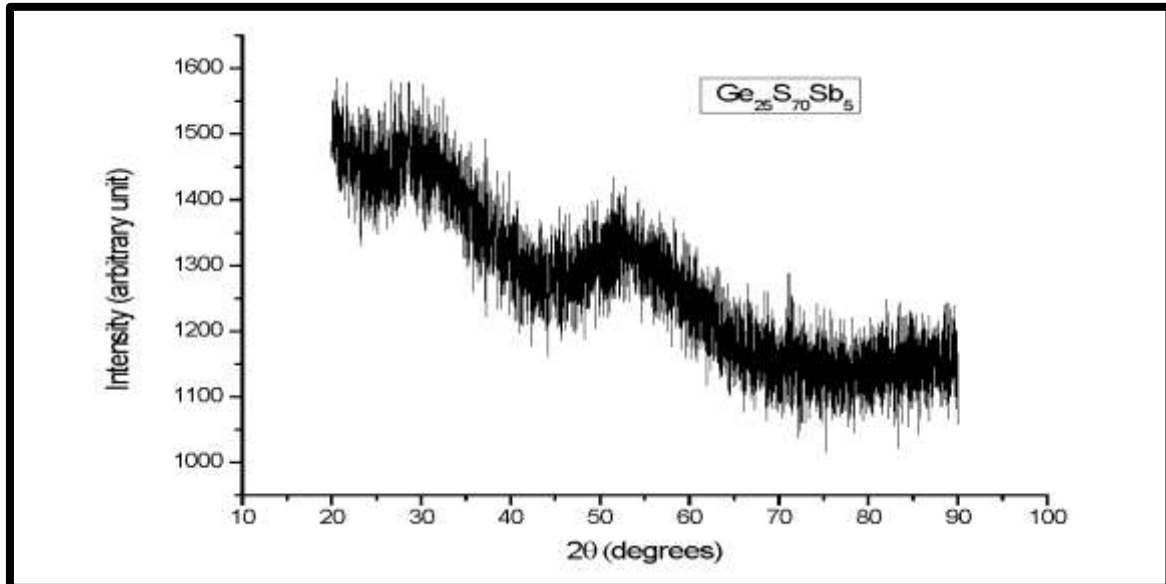


Figure 2: X Ray Diffraction pattern of GeSSb.

The bulk glassy samples Ge₂₅S₇₀-xSb_x (where x=0,5) were then used in Differential Scanning Calorimetry (MDSC 2920 TA instruments) in the Chemistry Bio-Chemistry lab of WPI, Worcester, MA, USA to run these samples at multiple ramp rates from 5 oC/min to 40 oC/min from 0 oC to 300 oC heat and cool. The respective heat flow of the samples was recorded with the variation of temperature and then plotted in the graph to see how these samples behave. Let’s call GeS as sample 1 (S1) and GeSSb as sample 2 (S2).

III. Theory and Results:

Theory Section:

To understand DSC results of IGTs for both samples S1 and S2, following theories are used in this paper.

1. Kinetic Model:

Following Arrhenius theory or kinetic theory model as mentioned in the published article [24-26], effect of ramp rates can be seen in these glassy alloys:

$$\beta = \beta_0 e^{\frac{-E_a}{RT}} \quad 1$$

Where β is ramp rate, β_0 is a constant, E_a , R, and T are activation energy, universal gas constant, and temperature respectively.

2. Gaussian Model of IGT peaks.

To analyze peaks observed in heating of DSC curves for these glassy alloys, Gaussian analysis is done, and peak details are found from Gaussian theory as mentioned in this publication [27].

The general Gaussian Equation can be given as:

$$f(x) = a \exp \left[-\frac{(x-b)^2}{2c^2} \right] + d \quad 2$$

Where a, b, c, d are parameters and they can be described as the parameter a is the height of the peak, b is the center of the peak position or peak value, c is the width of the peak, and d is the Asymptotic value that approaches far from the peak. It can be zero as well. The relationships between these parameters a, b, c, d and function $f(x)$ can be seen in the Figure 3 taken from this publication [27].

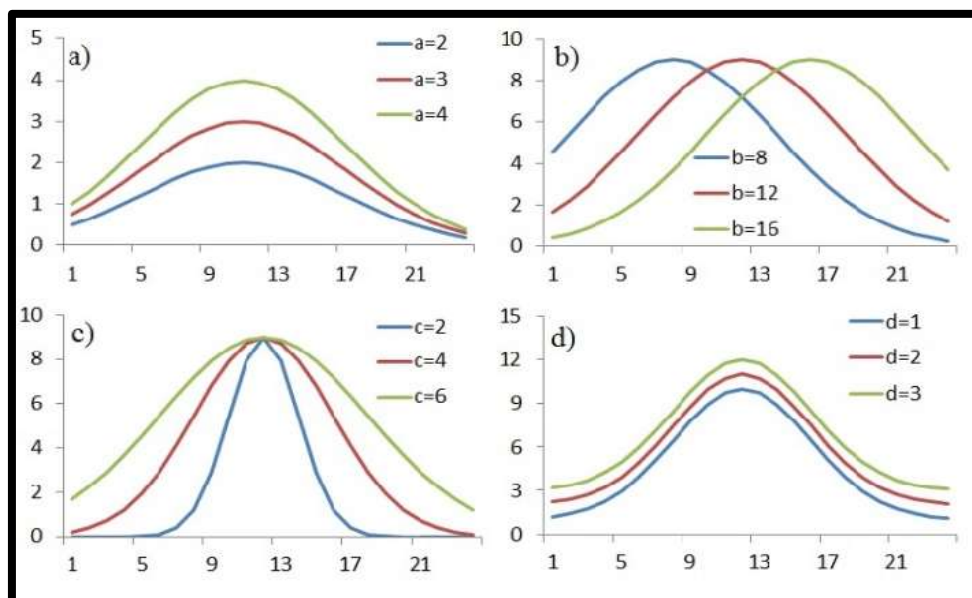


Figure 3: The meaning of Gaussian variables and constants explained by Yan GE et al published in a conference in 2015, taken from this publication [27]. This figure is showing how shape, size and position of exothermic peak changes as variable changes in Gaussian equation.

DSC Results Section:

The DSC results obtained for these glassy alloys can be divided into two parts of results as 1) Heat and Cool Effect on Samples, and 2) Ramp Rate effect on Samples.

1)Heat and Cool Effect on Samples:

The results obtained from DSC for GeS and GeSSb can be seen in Figure 4 that shows heat and cool of both samples at the same rate from 0 oC to 300 oC for heat and cool. It can be seen that a few small endothermic features appeared for both samples in heating only whereas nothing appeared in cooling for both. The two samples S1 (parent sample) and S2 with $x = 0$ and $x = 5$ for Sb showed some tiny endothermic features around 70-120 oC and nothing before and after in heating. These tiny features can be named as “Induced Glass Transitions” (IGTs) for these two samples. Usually, chalcogenide glasses show a big endothermic peak on heating as glass transition and then an exothermic peak as crystallization [20] and then a bigger endothermic peak as melting transition on heating[20] but in this case, none of these types of transitions are observed. Only small features are observed as multiple endothermic peaks on heating instead of getting only one endothermic peak on heating. Hence, we prefer to call them as Induced Glass Transitions (IGTs).

The parent sample S1 shows three dips with different sizes and shapes in heating from 70-120 oC whereas Sb doped glassy alloy with 5% of Sb, S2, shows reduced 3 dips from 70 – 120 oC those are smaller in size than as appeared in S1. It can be seen in Figure 5. Figure 5 is plotted as heat flow versus temperature plot for these samples.

To see clear dips in these samples from DSC curve, zoomed in graphs are plotted for these samples individually. These dips can be seen as three individual endothermic small peaks in heating in Figure 6. Figure 6 is plotted as heat flow normalized by the mass of the sample verses temperature. Sample 1 shows deeper endothermic peaks whereas Sample 2 shows shallower endothermic peaks. S1 is shown in Black and S2 is shown in Red. Tg1, Tg2, Tg3 are three induced glass transitions (IGTs) in these samples.

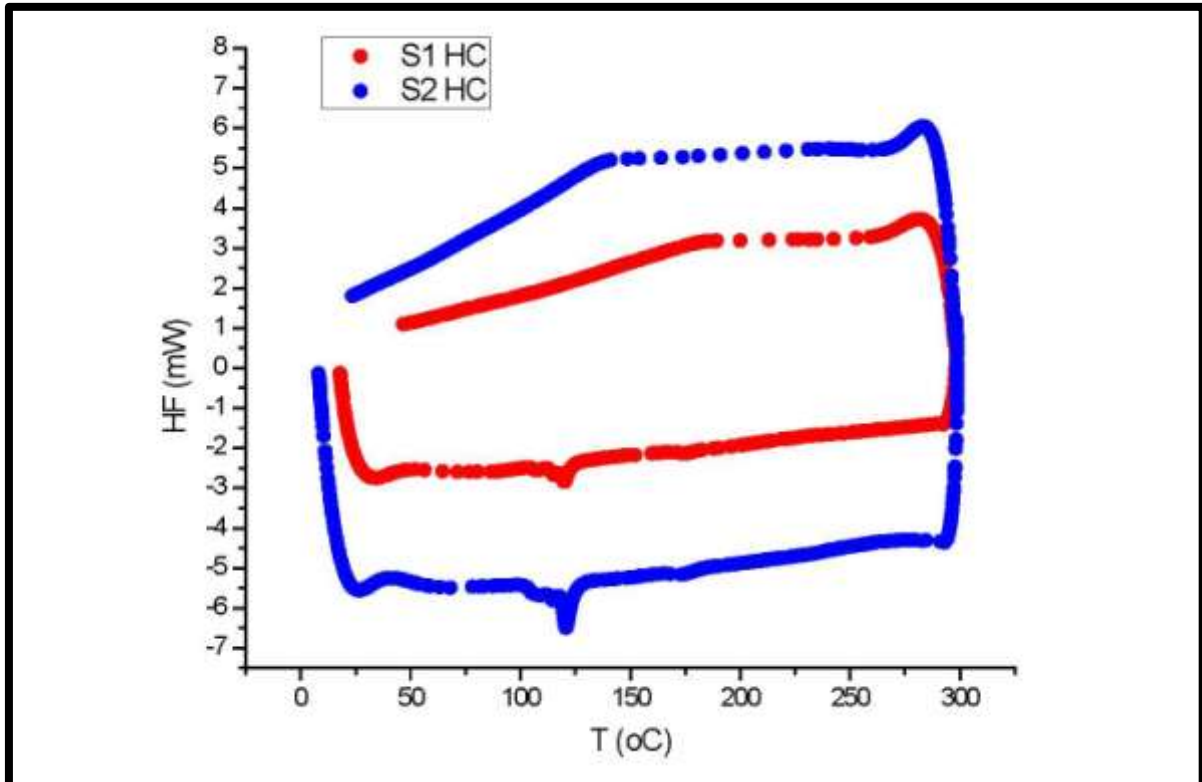


Figure 4: DSC curve of GeS(S1) and GeSSb(S2) samples from 0 °C to 300 °C showing heat and cool (HC) and the presence of Induced Glass Transitions at ramp rate 25 °C/min.

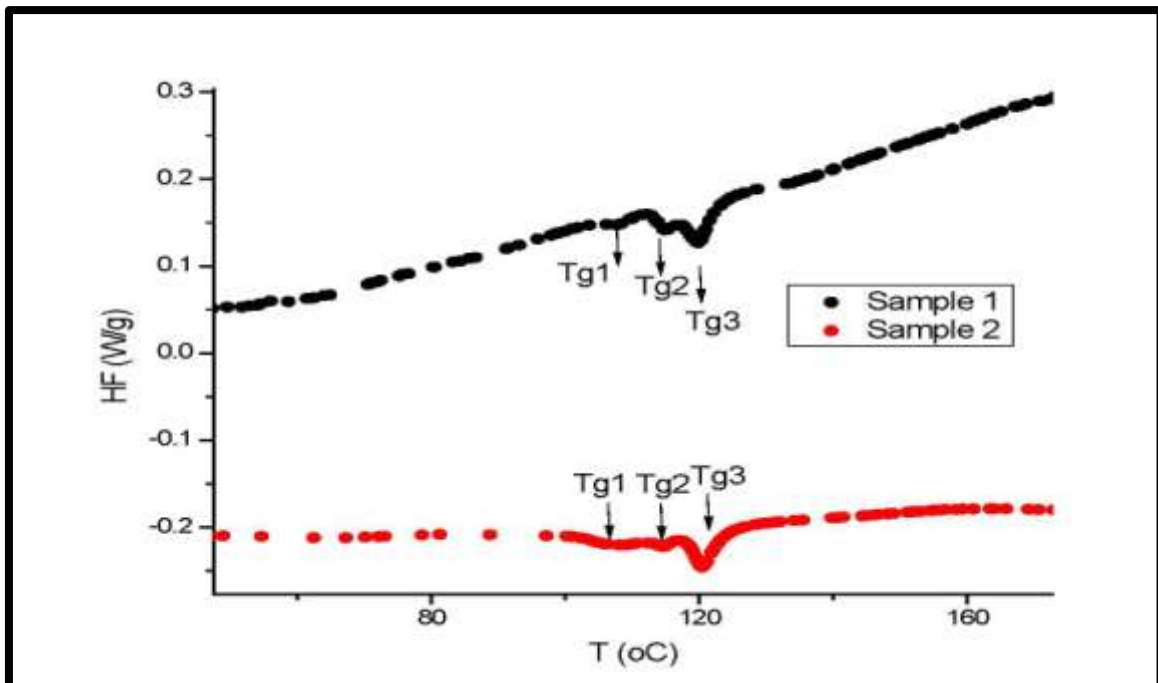


Figure 5: Zoomed in graphs of S1 and S2 for heat only showing as heat flow (normalized with mass) versus temperature at ramp rate 25 °C/min. Induced Glass Transitions (IGT) shown as Tg1, Tg2, Tg3 can be seen in the graph.

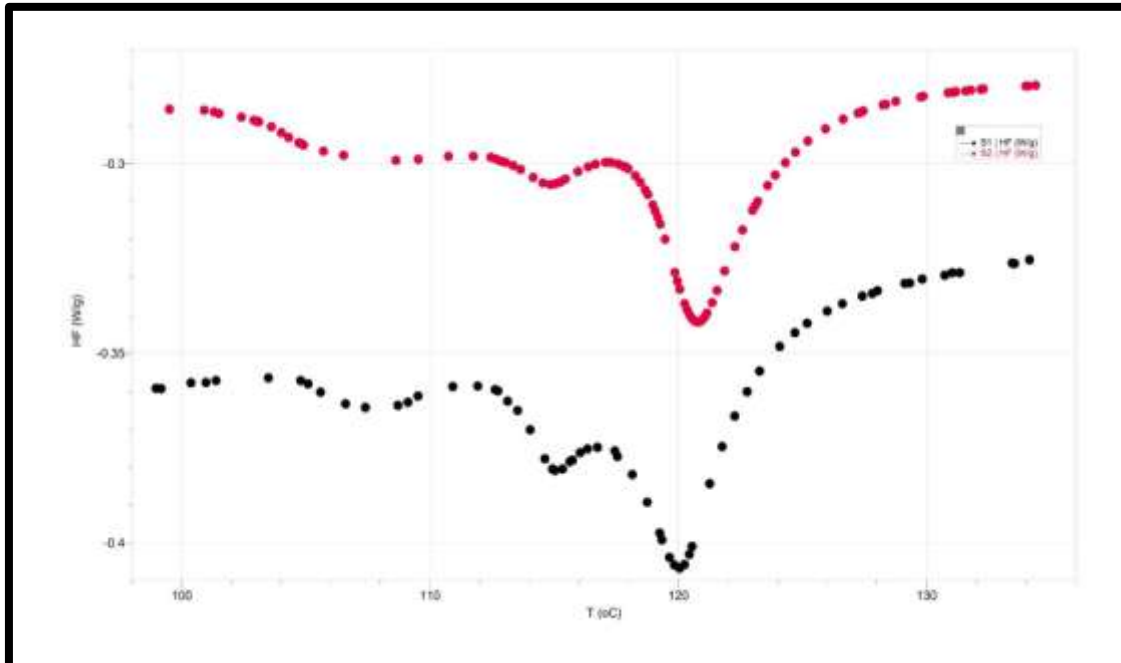


Figure 6: More zoomed in graphs of S1 (Black) and S2 (Red) for heat only showing as heat flow versus temperature at ramp rate 30 oC/min to show clear endothermic peaks for IGTs.

It can be seen easily that peak size, shape and position are changing when Sb is added. To understand further details of the shape, size, position and dynamics of these IGT peaks of S1 and S2, multi peak analysis is done using Gaussian Law. The detailed peak analysis of S1 is shown in Figure 7.

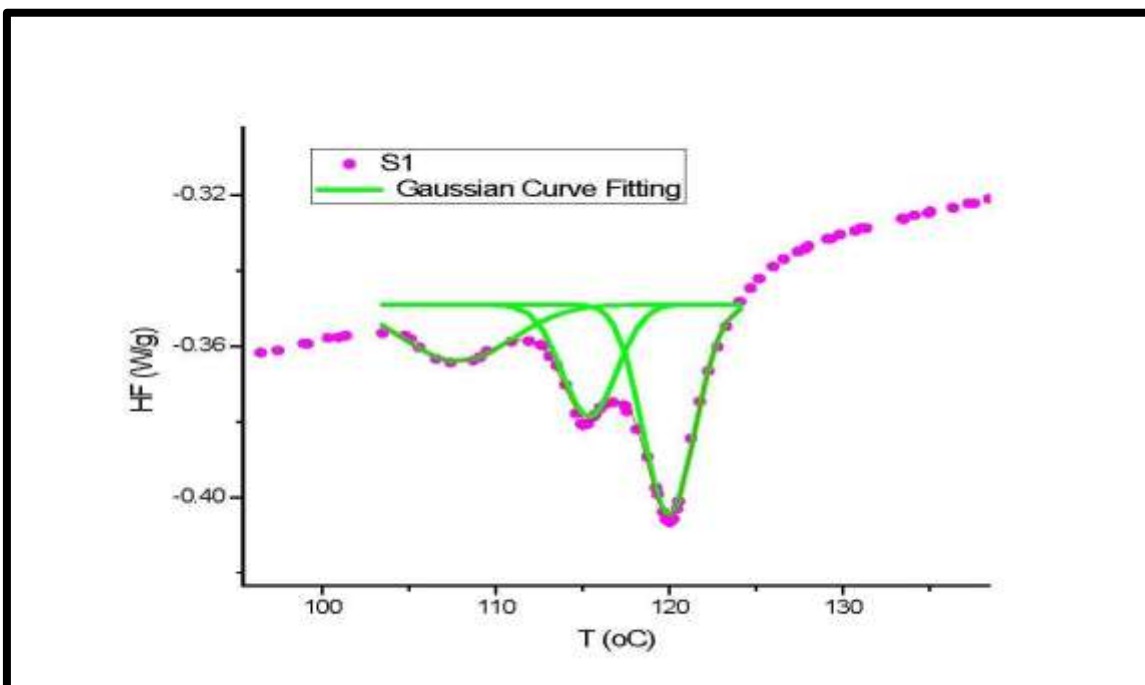


Figure 7: Gaussian Analysis of the endothermic peaks of S1 showing details of all three IGTs in heating.

Based on the Gaussian explanation shown in the theory section and by Figure 3 as can be seen in Yan GE et al, the IGT peaks obtained for GeSSb for this paper for S1 and S2 can be explained using Gaussian model equation. The detailed Gaussian Analysis is performed of all three peaks of IGTs of both samples S1 and S2 individually and shown in Figure 8.

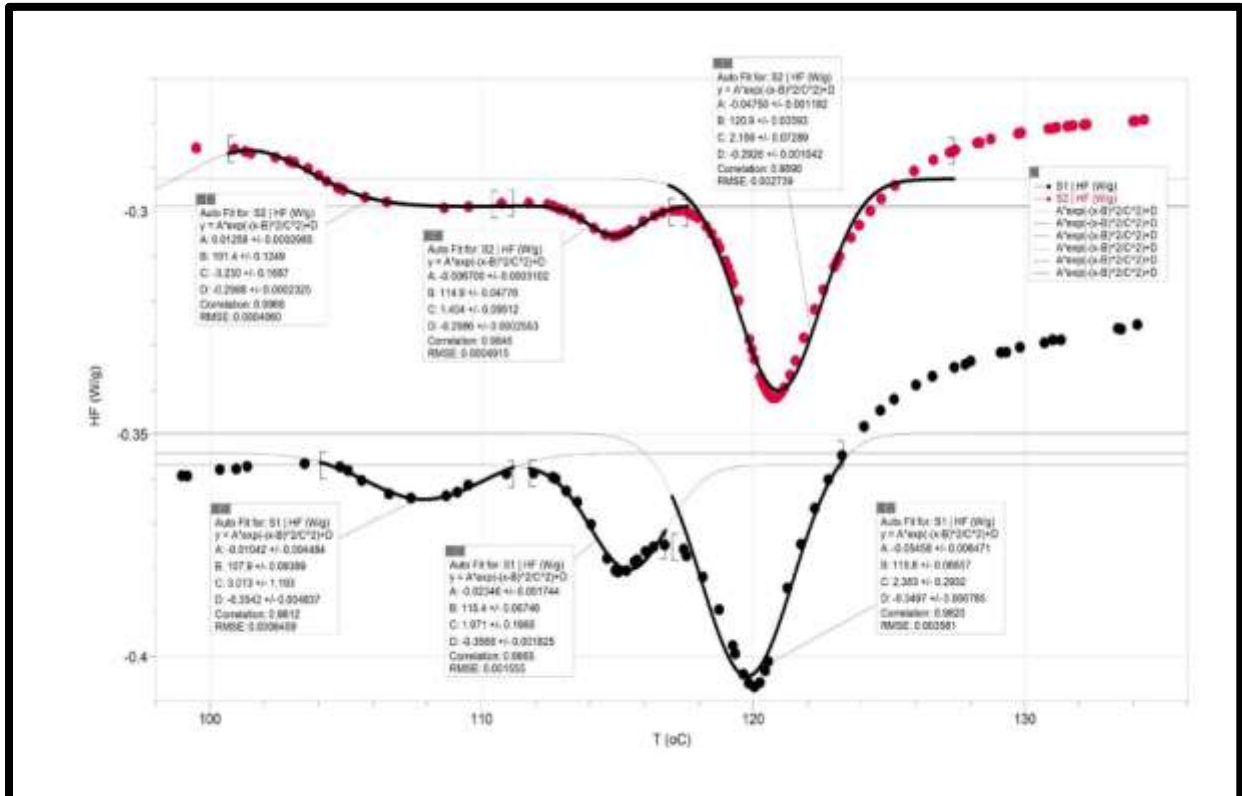


Figure 8: Gaussian Analysis of all three peaks of IGTs of S1 (Black) and S2 (Red) in detail.

Peak analysis provides details of the size, width, height, area of the peak and peak position as temperature is changing when Sb is absent or present by 5 % for S1 and S2. The data details of the peaks of S1 and S2 can be seen in Table 1 and Table 2.

Based on Gaussian peak analysis and enthalpies of each IGT peak, it can be seen that S1 has three endothermic peaks where the last peak, Tg3, is largest among them and similarly S2 also shows three IGT peaks and S2 also shows Tg3 as the largest peak. When IGT peaks are compared between S1 and S2, the first two Tg1 and Tg2 are found larger in S1 but smaller and shallower in S2 whereas the last peak Tg3 is found larger in S2 than S1 as shown in Figure 8.

Following Gaussian analysis of IGT peaks, the values obtained for 1stTg in S1 is shown below with possible uncertainty in the values obtain for peak 1 for S1.

$$y = f(x) = A * \exp(-(x-B)^2/C^2) + D$$

A: -0.01042 +/- 0.004484
 B: 107.9 +/- 0.09369
 C: 3.013 +/- 1.193
 D: -0.3542 +/- 0.004837
 Correlation: 0.9812
 RMSE: 0.0006459

Similar analysis is done for peak 1 of S2 and the values came as shown below:

$$y = f(x) = A * \exp(-(x-B)^2/C^2) + D$$

A: 0.01258 +/- 0.0002985
 B: 101.4 +/- 0.1249
 C: -3.230 +/- 0.1687
 D: -0.2988 +/- 0.0002325
 Correlation: 0.9968
 RMSE: 0.0004060

These are values of all parameters as mentioned in Gaussian model in the theory section for 1stTg for S1 and S2 respectively. These values can also be seen in Figure 8. When these values are compared, S1 has higher values than S2. The presence of Sb shrinks the Tg1 down and hence the values are smaller than S1.

It shows some material dynamics is taking place in S1 and S2 where these dynamics is bringing three IGT endothermic peaks in heating. As Sb is added to parent sample, S1, the effect of Sb makes Tg3 largest among all

peaks between both samples but makes Tg1 down and smaller as can be seen in Figure 9. The details of Gaussian data analysis can be seen in the Tables 1 and 2 below.

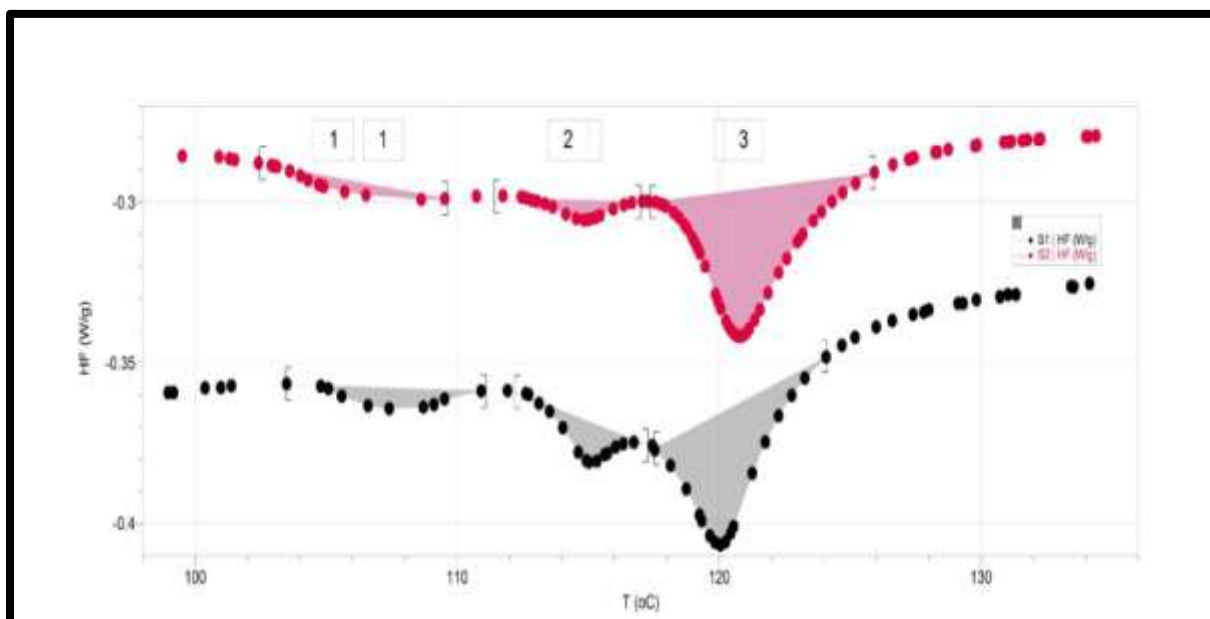


Figure 9: Area of each peak of IGTs for S1 and S2 showing endothermic energy involved in them.

In the Tables 1 and 2, H, w, Tp, A, dH, R and Cpp mean height, width, peak temperature, area, enthalpy, ramp rate and specific heat capacity of the peak respectively.

Data Table 1: Data details of the Gaussian Analysis and Peaks of the Sample 1.

S1	Tg1		Tg2		Tg3	
	Value	Uncertainty	Value	Uncertainty	Value	Uncertainty
H(W/g)	-0.01	+/- 0.004	-0.020	+/- 0.002	-0.055	+/- 0.006
w(oC)	3.01	+/- 1.193	1.970	+/- 0.198	2.383	+/- 0.293
Tp(oC)	107.90	+/- 0.094	115.4	+/- 0.067	119.800	+/- 0.067
A(WoC/g)	5.50	N/A	3.770	N/A	4.920	N/A
dH(J/g)	11.00	N/A	7.540	N/A	9.840	N/A
R(oC/min)	30.00	N/A	30.00	N/A	30.00	N/A
C _{pp} (J/g)	0.74	N/A	0.76	N/A	0.84	N/A

Data Table 2: Data details of the Gaussian Analysis and Peaks of the Sample 2.

S2	Tg1		Tg2		Tg3	
	Value	Uncertainty	Value	Uncertainty	Value	Uncertainty
H(W/g))	0.013	+/- 0.001	-0.007	+/- 0.001	-0.048	+/- 0.001
w(oC)	-3.23	+/- 0.169	1.404	+/- 0.095	2.159	+/- 0.073
Tp(oC)	101.4	+/- 0.125	114.9	+/- 0.048	120.9	+/- 0.036
A(WoC/g)	4.22	N/A	3.36	N/A	5.23	N/A
dH(J/g)	8.44	N/A	6.72	N/A	10.46	N/A
R(oC/min)	30.00	N/A	30.00	N/A	30.00	N/A
C _{pp} (J/g)	0.58	N/A	0.62	N/A	0.68	N/A

2)Effect of Ramp Rates on IGTs of the Samples:

The GeS and GeSSb samples are also studied for various heating rates. When S1 and S2 are heated with different ramp rates from 5 oC/min to 40 oC/min for same temperature range in DSC, it is found that each IGT

peak in both samples shift in temperature and shows rate kinetics. To study further in detail, zoomed in graphs are plotted for various ramp rates for S1 and S2 in Figure 10 and Figure 11.

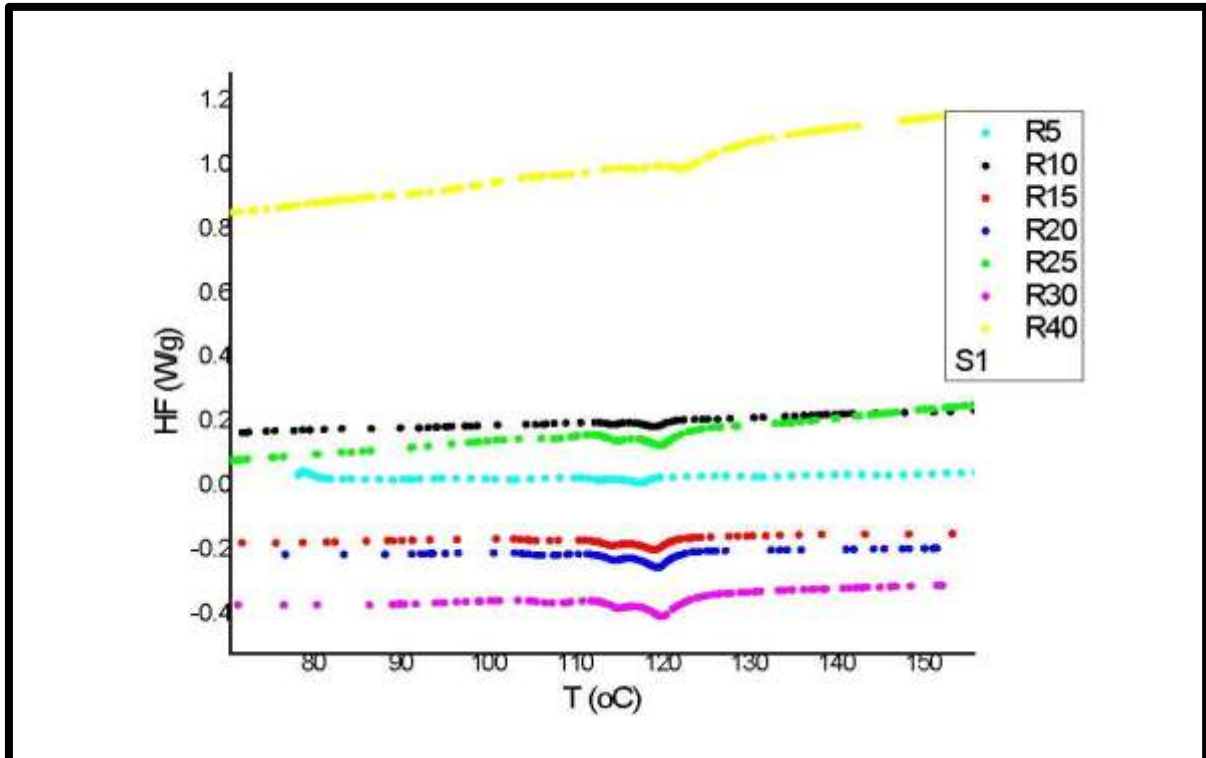


Figure 10: Effect of ramp rate of IGTs of S1.

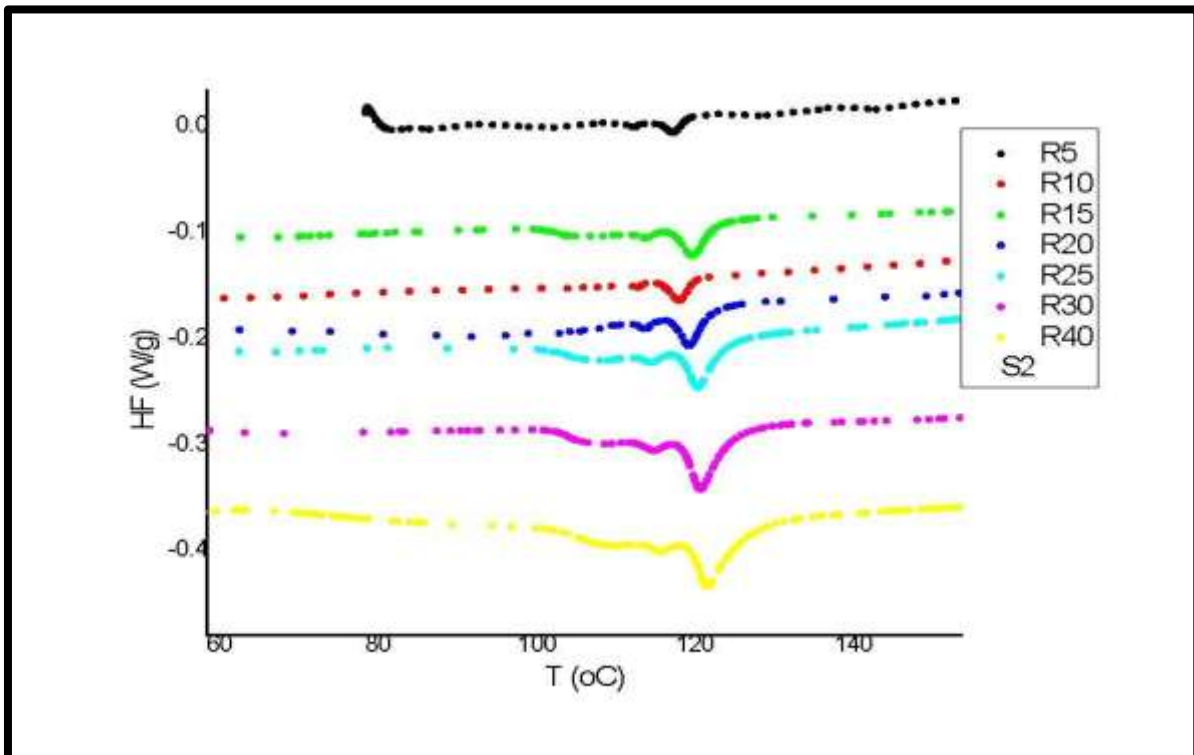


Figure 11: Effect of ramp rate of IGTs of S2.

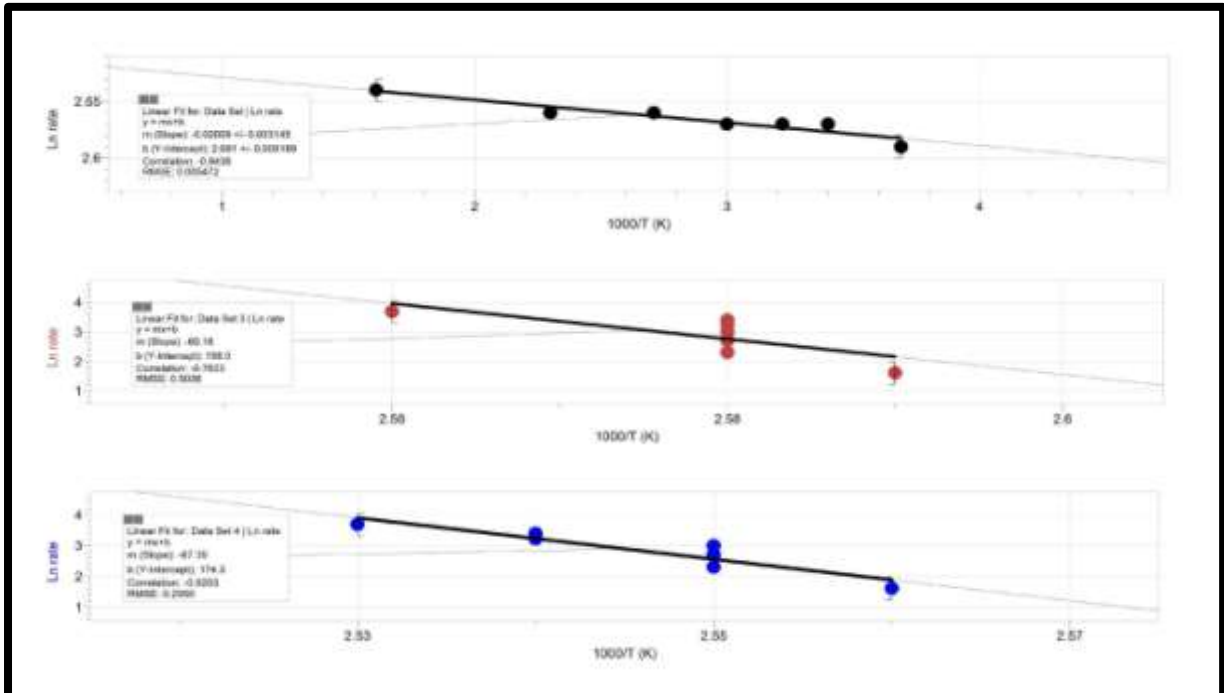


Figure 12: Ramp Rate Kinetics of IGTs of S1.

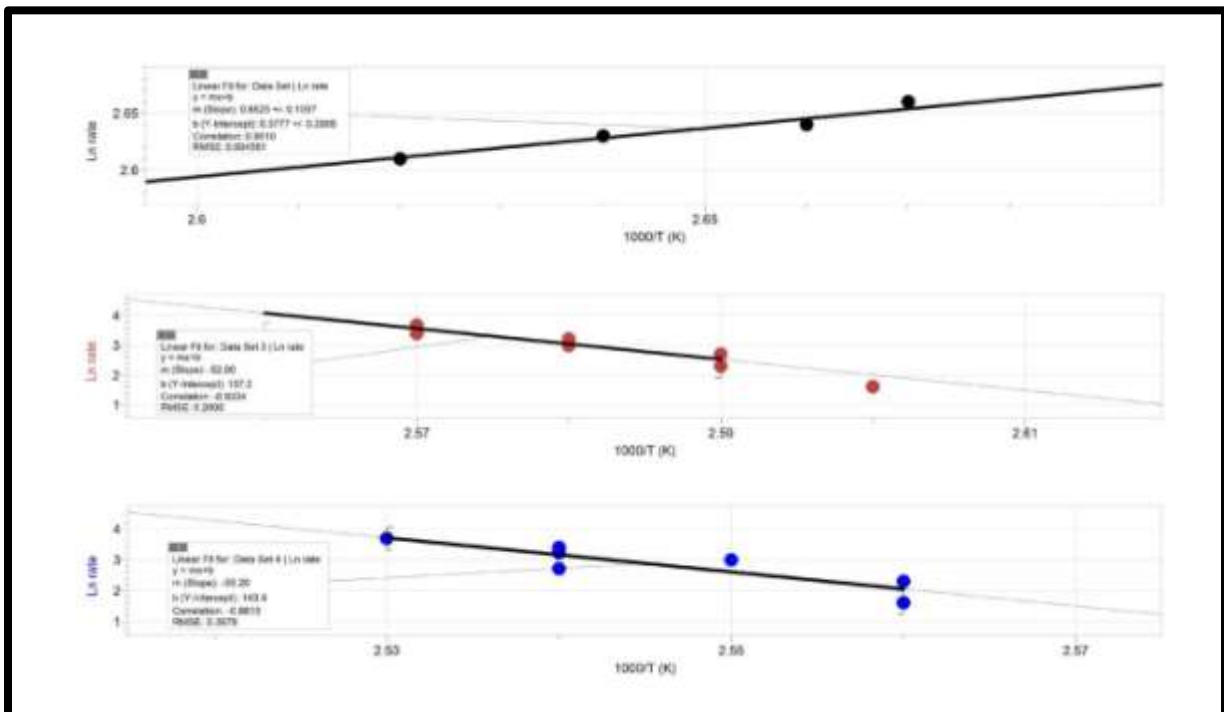


Figure 13: Ramp Rate Kinetics of IGTs of S2.

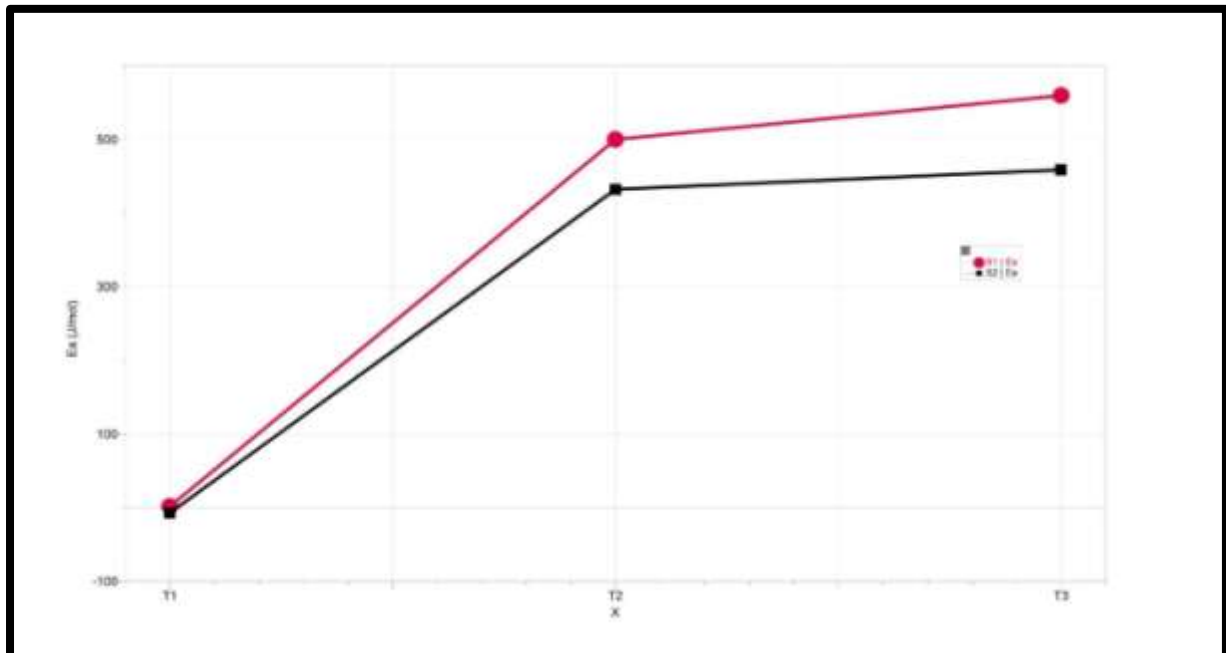


Figure 14: Variation of Activation energy of all IGTs of both samples S1(Red) and S2 (Black).

Following activated kinetic models and theories mentioned in the theory section and our previous publications [24-16], the activated kinetic graphs are plotted for these IGTs for S1 and S2 in Figures 12 and 13. These graphs show that both samples S1 and S2 shows kinetics in IGTs. All IGTs shift in temperature with ramp rates. Figure 14 shows a comparison between activation energies of IGTs for S1 and S2. It can be seen from Figure 14 that activation energies for S1 is higher than S2 for all IGTs.

Data details for all these IGTs as function of ramp rate is given below in Tables 3, 4, 5, 6 for both samples S1 and S2 respectively. It can be seen from Tables 3 and 4 that as ramp rate is increasing the T1, T2, T3 are moving forward in temperature for both samples but S2 is moving faster than S1. From Tables 5 and 6, it is clear that S1 has higher activation energy than S2. It means when Sb is added to the glassy alloy it flattens the peaks but also make them move faster with lower activation energy.

Data Table 3: Data details of ramp dependence of peaks of Sample 1.

Rate (oC/min)	T1 (oC)	T2 (oC)	T3 (oC)
5	103.27	112.83	117.79
10	105.10	114.23	119.19
15	105.40	114.51	119.26
20	106.40	114.65	119.61
25	107.60	114.86	119.89
30	107.80	115.14	120.08
40	109.40	117.54	122.78

Data Table 4: Data details of ramp dependence of peaks of Sample 2.

Rate (oC/min)	T1 (oC)	T2 (oC)	T3 (oC)
5	101.62	111.70	117.25
10	102.50	112.70	118.00
15	103.07	113.40	119.90
20	105.60	114.00	119.50
25	105.80	114.80	120.50
30	106.10	115.20	120.89
40	108.00	115.90	121.70

Data Table 5: Activation energy of all peaks of IGTs of Sample 1.

Sample 1	Ea (J/mol)	Uncertainty (J/mol)
T1	1.66	+/- 0.003
T2	500.10	+/- 22.85
T3	559.68	+/- 12.34

Data Table 6: Activation energy of all peaks of IGTs of Sample 2.

Sample 1	Ea (J/mol)	Uncertainty (J/mol)
T1	-7.06	+/- 0.11
T2	432.12	+/- 9.99
T3	458.71	+/- 13.71

IV. Discussion:

The DSC results of GeS and GeSSb samples show existence of three small endothermic peaks in heating those are Induced Glass Transitions (IGTs) where the first two peaks Tg1 and Tg2 are small but the third peak Tg3 is the largest one. The size, shape, position of peaks change as Sb is added to the parent sample. The first two peaks get shallower, and the third peak gets sharper and bigger with Sb. It represents that there are three types of activation taking place in these glassy alloys when they are heated. Since these glassy alloys are the combination of GeS, they show slow crystallization when they get heated and due to the slow process of crystallization, these glassy alloys do not show an exothermic peak in heating as crystallization as other typical chalcogenide glasses show. The unique and most interesting thing observed with these glass alloys is appearance of three tiny glass transitions on heating. It means the GeSSb sample show relaxation in three steps when they are heated in terms of three IGTs. The first two IGTs are smaller than the third one and the reason can be given as more heat goes into the samples, the molecules of the alloys get activated towards higher energy and show bigger dips in terms of larger induced glass transition. The effect of Sb makes the first two Tgs down as it suppresses the effect of GeS slow process and makes the third peak larger. It also shows lower activation energy than GeS sample.

Furthermore, it can be explained in terms of the density of material as well. As Sb is added to GeS alloy, the density of the parent sample (S1) changes. This change can be seen as following:

Density= Mass/Volume

For Ge25S75 glassy alloy (S1) the density can be given as

$$\rho = m/V = 5g/1.78036113646cc = 2.80841898 = 2.802 \text{ g/cc}$$

For Ge25S70Sb5 glassy alloy (S2) the density can be given as

$$\rho = m/V = 5g/1.16110772464cc = 4.30597783 = 4.306 \text{ g/cc}$$

The density results shows that density increases due to the doping of ternary element Sb in GeS glassy system, thus there is generation of opposite behavior in doped samples, the doping of ternary component also resulted in the change of measured glass transition temperatures.

For the GeS based glasses a 'model' base glass is used to compare the changes in the local electron density around germanium atom and the changes in the ratio of medium to short range order, when the ternary element is doped. Due to this change GeSSb shows higher Tg3 than GeS on heating.

V. Conclusion:

This study explores detailed thermal results of two chalcogenide GeSSb glassy alloys using Differential Scanning Calorimetry (DSC) technique. The two bulk samples of Ge25S75-xSbx (where x = 0% and 5%) were used to run from 0 oC to 300 oC on heat and cool varying ramp rates from 5 oC/min to 40 oC/min in DSC. These glassy alloys show three unique Induced Glass Transition (IGTs) peaks as endothermic peaks on heating. They do not show any crystallization peak on heating which is unusual for chalcogenide glasses unless they show slow crystallization which slows down the process of crystallization. In GeS glasses, it is observed that some of the compositions show slow crystallization, but no one has reported multiple glass transitions in heating. These glassy alloys are unique as they showed three glass transitions on heat and shows that molecular arrangement process in these glassy alloys is so slow that they can show three step glass transitions with three activation energies. In the presence of Sb, the density increases, hence the third glass transition increases and the process become slower that results in low activation energy.

Acknowledgement:

Authors like to acknowledge Professor John C. MacDonald from the department of Chemistry and Biochemistry of WPI, Worcester, MA, USA for letting us use his laboratory with Differential Scanning

Calorimetry (DSC) model MDSC 2920 from TA instruments for DSC data. Authors like to thank to TA instruments for providing cups and lids for these experiments. Last but not the least, Om, a high school student, should be acknowledged for doing some part of data analysis of this paper as his summer research program.

References:

- [1]. L. Li, H. Lin, S. Qiao, Y. Zou, S. Danto, K. Richardson, J. D. Musgraves, N. Lu, J. Hu, Integrated flexible chalcogenide glass photonic devices, *Nat. Photonics*, 8 (2014) 643–649.
- [2]. Anjani Kumar, R.K. Shukla, A. Kumar, Rajeev Gupta, *Infrared Physics & Technology*, 102, (2019) 103056 (1-7)
- [3]. C.C. Huang, C.C. Wu, K. Knight, D.W. Hewak, Optical properties of CVD grown amorphous Ge-Sb-S thin films, *Journal of Non-crystalline Solids* 356 (2010) 281-285.
- [4]. N. Mehta, A. Kumar, Recent advances in chalcogenide glasses for multifunctional applications in fiber optics, *Recent Patents Mater. Sci.* 6 (2013) 59-67
- [5]. Evaluation of nonlinear optical parameters of $\text{Se}_{40}\text{As}_{60-x}\text{S}_x$ ($x=10, 20$) chalcogenide thin films for photonic applications, Anjani Kumar, S. Shukla, R. K. Shukla, Rajeev Gupta, *Indian Journal of Physics*, <https://doi.org/10.1007/s12648-022-02454-5>, 2022.
- [6]. K. Tanaka, K. Shimakawa, *Phys. Status solidi B*, 246(8) (2009) 1744-57.
- [7]. P. Damian San-Roman-Alerigi, D. H. Anjum, Y. Zhang, X. Yang, A. Benslimane, T. K. Ng, Md. Alsunaidi, B. S. Ooi, *J. Appl. Phy.*, 113 (2013) 044116.
- [8]. M. Buffiere, D. S. Dhawale, F. El-Mellouhi, *Energy Technology*, chalcogenide materials and derivatives for photovoltaic applications, 7(2019) 1900819.
- [9]. D.J. Milliron, S. Raoux, R.M. Shelby, J. Jordan-Sweet, Solution-phase deposition and nanopatterning of GeSbSe phase-change materials., *Nat. Mater.* 6 (2007) 352–356.
- [10]. Mohsin Ganai, M. Zulfeqar, Effect of Zinc additive on dielectric properties of Cd-Se glassy system, *Progress in Natural Science: Materials International* 25 (2015) 222-228.
- [11]. Ho Soonmin, I. Paulraj, Mohanraj Kumar, Rajesh K. Sonkar, P. Nandi, Recent developments on the properties of chalcogenide thin films, (2022) a book chapter. (DOI: 10.5772/intechopen.102429).
- [12]. El-Sayed, M. Farg, Optical properties of amorphous $\text{Ge}_{30-x}\text{Sb}_x\text{S}_{70}$ films, *Optics & Laser Technology*, 38 (2006) 14-18.
- [13]. J.C. Phillips, Topology of covalent non-crystalline solids I: Short range order chalcogenide alloys, *J. non-crystalline solids*, 13, 4 (1979), 153-181.
- [14]. R. S. Tewari, N. Mehta, R. K. Shukla, A. Kuma, Thermal characterization of some Se-Ge-In chalcogenide glasses by differential scanning calorimetry, *European Journal of Glass Science and Technology Part B Physics and Chemistry of Glasses*, 46, 6 (2005), 595-599.
- [15]. Oweimreen, G., & Morsy, M. (2000). DSC studies on p-(n-alkyl)-p'-cyanobiphenyl (RCB's) and p-(n-alkoxy)-p'-cyanobiphenyl (ROCB's) liquid crystals. *Thermochimica Acta*, 346(1–2), 37–47. [https://doi.org/10.1016/s0040-6031\(99\)00411-6](https://doi.org/10.1016/s0040-6031(99)00411-6)
- [16]. D. Sharma, J.C. MacDonald, A. Kumar, R.K. Shukla, Effect of Fast Scanning Calorimetry (FSC) on Crystallization of Se 90 In 8 Ag 2 Glassy Alloy, *Materials Focus* 7, 1(2018), 89-93.
- [17]. Sharma, D., MacDonald, J. C., & Iannacchione, G. S. (2006, August 1). Thermodynamics of Activated Phase Transitions of 8CB: DSC and MC Calorimetry. *The Journal of Physical Chemistry B*, 110(33), 16679–16684.
- [18]. Sharma, D. (2010, May 18). Non-isothermal kinetics of melting and nematic to isotropic phase transitions of 5CB liquid crystal. *Journal of Thermal Analysis and Calorimetry*, 102(2), 627–632. <https://doi.org/10.1007/s10973-010-0837-2>
- [19]. Sharma D. Calorimetric study of activated kinetics of the nematic and smectic phase transitions in an aligned nano-colloidal liquid crystal + aerosil gel. *J Therm Anal Calorim.* 2008;93:899–906.
- [20]. Sharma, D., Shukla, R. K., Singh, A., Nagpal, A. K., & Kumar, A. (2000). Effect of Ag addition on glass transition and crystallization in $\text{Se}_{80}\text{Te}_{20}$ glass. *Advanced Materials for Optics and Electronics*, 10(6), 251–259.
- [21]. Sharma, D., & Mello, J. (2022a). Effect of Reheating and Ramp Rates on Phase Transitions of 5OCB Liquid Crystal using Logger Pro. *International Journal of Research in Engineering and Science (IJRES)*, 10(9), 218–236.
- [22]. Sharma, D., MacDonald, J. C., & Iannacchione, G. S. (2006a). Role of Aerosil Dispersion on the Activated Kinetics of the $\text{LC}_{1-x}\text{Si}_x$ System. *The Journal of Physical Chemistry B*, 110(51), 26160–26169. <https://doi.org/10.1021/jp065209z>
- [23]. Sharma, D., Iannacchione, G. S. (2007) Kinetics of Induced Crystallization of the $\text{LC}_{1-x}\text{Si}_x$ System. *The Journal of Physical Chemistry*, 111(8), 1916-1922. <https://doi.org/10.1021/jp067736o>
- [24]. Johnson, W.A., Mehl, R.F. (1939). Reaction Kinetics in Processes of Nucleation and Growth. *Transactions of the American Institute of Mining and Metallurgical Engineers*, 135, 416-442.
- [25]. Avrami, M. (1939). Kinetics of Phase Change. I General Theory. *The Journal of Chemical Physics*, 7(12), 1103–1112. <https://doi.org/10.1063/1.1750380>
- [26]. Avrami, M. (1940). Kinetics of Phase Change. II Transformation- Time Relations for Random Distribution of Nuclei. *The Journal of Chemical Physics*, 8(2), 212–224. <https://doi.org/10.1063/1.1750631>
- [27]. Yan Ge, J. Dai, K Qian, D. Hepburn, C. Zhou, Simulation of domestic electricity load profile by multiple Gaussian Distribution, 23rd international conference on electricity distribution, Lyon, 15-18 Jun 2015, paper 0107.